Tropolone as High-Performance Robust Anchoring Group for Dye-Sensitized Solar Cells

Tomohiro Higashino, Yamato Fujimori, Kenichi Sugiura, Yukihiro Tsuji, Seigo Ito, and Hiroshi Imahori*

Abstract: Tropolone has been employed for the first time as an anchoring group for dye-sensitized solar cells (DSSCs). The DSSC based on a porphyrin with the tropolone moiety, **YD2-*o*-C8T** exhibited a power conversion efficiency of 7.7%, which is almost comparable to a reference porphyrin with a conventional carboxylic group, **YD2-*o*-C8**. More importantly, **YD2-*o*-C8T** was found to display the superior DSSC durability as well as binding ability to TiO_2 to **YD2-*o*-C8**. These results unambiguously demonstrate that tropolone is the highly promising anchoring group of any dyes for DSSCs in terms of device durability as well as photovoltaic performance.

In recent years, the increasing energy consumption and concern about environmental issues strongly demand utilization of sunlight as alternative, clean and infinite energy source. From this point of view, photovoltaic devices are expected as promising technologies that directly convert solar energy into electricity. Since the pioneering work by Grätzel and co-workers in 1991,[1] dye-sensitized solar cells (DSSCs) have attracted a great deal of attention as an alternative to silicon-based solar cells owing to their low-cost production and high power conversion efficiency (η). Various organometallic/organic dyes have been explored for their application to DSSCs.[2–5] For instance, porphyrins are regarded as a promising candidate because of their intense absorption in the visible and near-infrared (NIR) regions, and versatile molecular design.[4] Indeed, push-pull type porphyrin sensitizers have realized their excellent light-harvesting ability and demonstrated high η-values more than 10% in DSSCs application.[5]

To date, carboxylic acids such as benzoic acid and cyanoacrylic acid have been the most widely used anchoring group to a TiO_2 surface for DSSCs. However, carboxylic acids are prone to dissociate from the TiO_2 surface during the device operation. Considering the durability of DSSCs for practical application, such detachment of the adsorbed dye from the TiO_2 is undesirable.[6] For this reason, it is pivotal to develop a novel anchoring group with higher binding ability to the TiO_2 surface than conventional carboxylic acid. He and co-workers found that 8-hydroxyquinoline (HOQ) is an attracting candidate to replace the benzoic acid group.[7] Although the η-value of DSSC based on the HOQ-modified porphyrin was moderate, it displayed a higher stability on TiO_2 than its analogue with benzoic acid as the anchoring group.

Tropolones are well-known compounds that can be easily synthesized and form stable complexes with various metal ions.[8] A resonance structure, aromatic tropylium ion, contributes to the electronic structure of tropolones (Figure 1). In this respect, tropolones can act as an electron-withdrawing motif in π-system. Reports utilizing tropolones as the key motif of functional molecules are still limited, whereas metal complexes of tropolones have been employed as building blocks for supramolecular coordination complexes[9] and stable liquid crystals.[10] For instance, Shionoya and co-workers used tropolone as a bidentate ligand to construct the stable high-order structure of multinuclear complexes.[9a] They revealed higher stability of tropolone-Ti^{IV} complex than HOQ-Ti^{IV} complex. Thus, we envisioned that the tropolone moiety would be suitable for anchoring dyes to TiO_2 robustly. Herein, we report the first use of tropolone as the anchoring group of the dye for DSSCs. Representative porphyrin sensitizer **YD2-*o*-C8** was chosen as a reference[5b] and the benzoic acid was replaced with the tropolone moiety to yield **YD2-*o*-C8T** for the comparison of their photovoltaic performances and device durability (Figure 1).

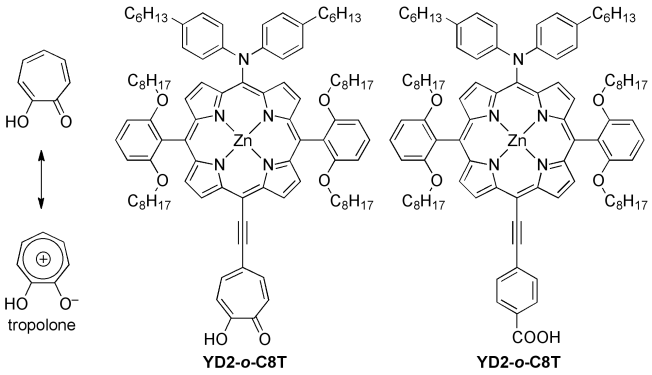

Figure 1. Resonance structure of tropolone and molecular structures of porphyrins.

The synthetic route of **YD2-*o*-C8T** was illustrated in Scheme 1. Reference porphyrin, **YD2-*o*-C8**, and porphyrin precursor **1** were synthesized according to literature.[5b] Deprotection of **1** with tetrabutylammonium fluoride (TBAF) and subsequent Sonogashira coupling with 5-iodo-2-methoxytropone[11] provided tropolone ether **2** in 90% yield. The reaction of **2** with potassium hydroxide furnished **YD2-*o*-C8T** in satisfactory yield (42%). Repeated reprecipitation of **YD2-*o*-C8T** from CH_2Cl_2/acetonitrile was necessary for the sufficient purification due to severe adsorption of the tropolone moiety on silica-gel for column chromatography. Details of the synthesis

[*] Dr. T. Higashino, Y. Fujimori, K. Sugiura, Y. Tsuji, Prof. Dr. H. Imahori
Department of Molecular Engineering, Graduate School of Engineering, Kyoto University
Nishikyo-ku, Kyoto, 615-8510 (Japan)
E-mail: imahori@scl.kyoto-u.ac.jp

Prof. Dr. S. Ito
Graduate School of Engineering, University of Hyogo
2167 Shosha, Himeji, Hyogo, 671-2280 (Japan)

Prof. Dr. H. Imahori
Institute for Integrated Cell-Material Sciences (WPI-iCeMS)
Kyoto University
Nishikyo-ku, Kyoto, 615-8510 (Japan)

Supporting information for this article is given via a link at the end of the document.

and characterization are described in Supporting Information (Figures S1-S3).

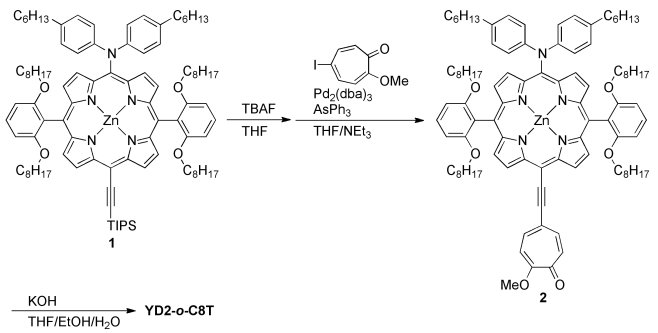

Scheme 1. Synthesis of **YD2-*o*-C8T**.

The UV/vis absorption spectra of **YD2-*o*-C8T** and **YD2-*o*-C8** in THF are displayed in Figure 2. The Soret and Q bands of **YD2-*o*-C8T** are shifted toward longer wavelength than those of **YD2-*o*-C8**, demonstrating the higher light-harvesting ability of **YD2-*o*-C8T** than **YD2-*o*-C8** in the visible region owing to the enhanced push-pull character. The steady-state fluorescence spectra were also measured in THF (Figure S4). From the intersection of the normalized absorption and fluorescence spectra, the zero-zero excitation energies (E_{0-0}) were calculated to be 1.86 eV for **YD2-*o*-C8T** and 1.89 eV for **YD2-*o*-C8**.

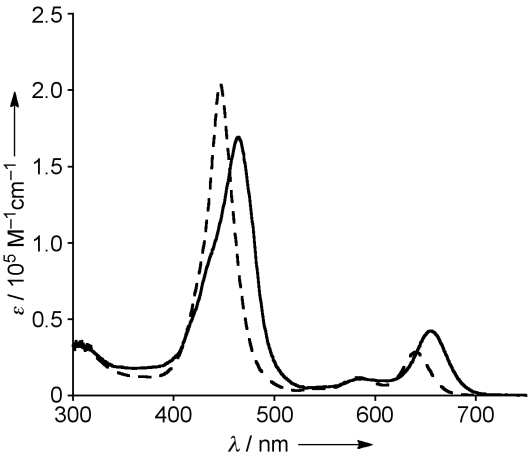

Figure 2. UV/Vis absorption spectra of **YD2-*o*-C8T** (solid line) and **YD2-*o*-C8** (dashed line) in THF.

Electrochemical properties were studied by differential pulse voltammetry (DPV) in THF versus NHE with tetrabutylammonium hexafluorophosphate as an electrolyte (Table 1 and Figure S5). The first oxidation potential (E_{ox}) of **YD2-*o*-C8T** (0.79 V) is almost the same as **YD2-*o*-C8T** (0.81 V), whereas the first reduction potential (E_{red}) of **YD2-*o*-C8T** (–1.14 V) is shifted to a positive direction by 0.12 V than that of **YD2-*o*-C8** (–1.26 V). This supports the higher electron-withdrawing ability of tropolone than benzoic acid. The electrochemical HOMO–LUMO gap of **YD2-*o*-C8T** (1.93 V) is smaller than that of **YD2-*o*-C8** (2.07 V), which agrees with the trend in the optical HOMO–LUMO gaps (Table 1). From the spectroscopic and electrochemical measurements, driving forces for electron injection (ΔG_{inj}) from the porphyrin excited singlet state to the conduction band (CB) of TiO_2 (–0.5 V vs NHE)[5c] and for reduction of the porphyrin radical cation (ΔG_{reg}) by a I^-/I_3^- redox couple (+0.4 V vs NHE)[5c] are calculated. Since these driving forces are more negative than –0.3 eV, electron injection and dye regeneration processes are exergonic and the driving forces are sufficient for efficient electron transfer.

Table 1. Electrochemical properties

dyes	E_{ox}[a] / V	E_{red}[a] / V	E_{0-0}[b] / eV	E^*_{ox}[c] / V	ΔG_{inj}[d] / eV	ΔG_{reg}[e] / eV
YD2-*o*-C8T	0.79	–1.14	1.86	–1.07	–0.57	–0.39
YD2-*o*-C8	0.81	–1.26	1.89	–1.08	–0.58	–0.41

[a] First oxidation and reduction potentials (vs. NHE). [b] Determined from the intersection of normalized absorption and emission spectra. [c] Determined by adding E_{0-0} to E_{ox} (vs. NHE). [d] Driving force for electron injection from the porphyrin excited singlet state to the CB of TiO_2 (–0.5 V vs. NHE). [e] Driving force for dye regeneration by I^-/I_3^- redox shuttle (+0.4 V vs. NHE).

To obtain the insight on ground-state geometry and electronic structures of the frontier orbitals of the porphyrins, we performed DFT calculations on the model porphyrins with B3LYP/6-31G(d) level (Figure S6).[12] Both the porphyrins display similar electron densities in the HOMO and LUMO as well as the ground-state geometry. The calculated HOMO–LUMO gaps of **YD2-*o*-C8T** and **YD2-*o*-C8** are determined to be 2.23 and 2.32 eV, respectively, which parallel with the optical and electrochemical HOMO–LUMO gaps. The electron density distribution on the oxygen atoms of the tropolone moiety in the LUMO of **YD2-*o*-C8T** is 2.8%, which is even higher than that of the carboxyphenyl moiety in the LUMO of **YD2-*o*-C8** (2.3%). Thus, the tropolone moiety ensures efficient electron injection and its robust binding to TiO_2.

At first, we examined the adsorption properties of the tropolone moiety on TiO_2 (Figure S7). A TiO_2 film was immersed into a 4:1 mixture of ethanol/toluene with 0.2 mM porphyrin to give a porphyrin-stained TiO_2 film. The porphyrin surface coverage (Γ) adsorbed on the TiO_2 film was determined by measuring the absorbance of the porphyrin that was dissolved from the porphyrin-stained TiO_2 film into an alkaline 1:1 mixture of THF/H_2O. During immersion, the porphyrins reveal almost identical adsorption profiles as a function of immersion time and reached the constant Γ-values on TiO_2 in 3 h. The saturated Γ values of 8.3×10^{-11} mol cm^{-2} for **YD2-*o*-C8T** and 8.5×10^{-11} mol cm^{-2} for **YD2-*o*-C8** are virtually the same. Taking into account the saturated, comparable Γ-values together with the dye sizes, both the porphyrins form well-packed monolayers on the TiO_2.

The FT-IR spectrum of **YD2-*o*-C8T** for the solid sample reveals characteristic peaks at 1585 cm^{-1} arising from ν(C=O) and around 1250 cm^{-1} arising from ν(O–H) and ν(C–O) (Figure

S8).[13] After the adsorption on TiO_2, the spectrum shows broadening of the peaks, which is seen for tropolone-metal bidentate complexes.[8] To gain further information on the binding mode, X-ray photoelectron spectroscopy (XPS) measurements were conducted for **YD2-*o*-C8T**-stained TiO_2 as well as the references (Figures S9–S11). The O1s photoelectron spectrum exhibits three oxygen peaks. The peak at 529.9 eV originates from oxygen atoms of the TiO_2 surface. The remaining peaks at 532.8 and 531.5 eV are ascribed to four oxygen atoms of the octyloxy moiety and two oxygen atoms of the tropolone moiety that binds to the TiO_2 surface, respectively. From these XPS measurements, combined with the FT-IR spectra, we assigned the binding mode of **YD2-*o*-C8T** on TiO_2 as symmetrical bidentate coordination.

Then, the photovoltaic properties of the porphyrin DSSCs were measured under standard AM 1.5 condition using an electrolyte solution containing I^-/I_3^- redox shuttle. To optimize the cell performances, we first examined the effect of immersion time (Figure S12). The DSSCs based on **YD2-*o*-C8T** and **YD2-*o*-C8** display the optimized η-values of 5.3 and 7.9% in immersion time of 3 and 4 h, respectively. By fixing the respective immersion time each porphyrin was also sensitized under various concentration of chenodeoxycholic acid (CDCA), co-adsorbent for the suppression of dye aggregation (Figure S13). However, the η-values decrease by the addition of CDCA, suggesting that the four octyloxy groups around the porphyrin core sufficiently inhibit dye-aggregation. The DSSCs were further kept under dark conditions to improve the cell performance. All the DSSCs attain the highest η-values after several days aging (Figure S14).[5c,14] The photocurrent-voltage characteristics of the DSSCs based on **YD2-*o*-C8T** and **YD2-*o*-C8** under the finally optimized conditions are depicted in Figure 3. The IPCE spectrum of the DSSC based on **YD2-*o*-C8T** exhibits photocurrent generation up to 800 nm, reflecting its higher light-harvesting ability than **YD2-*o*-C8**. Detailed photovoltaic parameters are listed in Table 2. The maximal DSSC performance of **YD2-*o*-C8T** (η = 7.7%) is slightly lower than that of **YD2-*o*-C8** (η = 8.8%). It is noteworthy that **YD2-*o*-C8T** achieved the highest η-value among porphyrin DSSCs where other anchoring groups except carboxylic acid were used.[7,15]

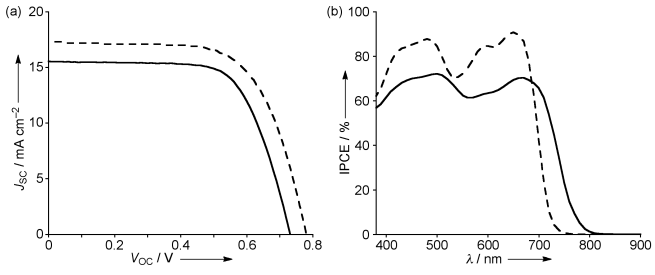

Figure 3. (a) Photocurrent-voltage characteristics and (b) photocurrent action spectra of the DSSCs based on **YD2-*o*-C8T** (solid line) and **YD2-*o*-C8** (dashed line).

Table 2. Photovoltaic performances[a]

dyes	J_{SC} / mA cm^{-2}	V_{OC} / V	ff	η / %
YD2-*o*-C8T	15.6 (15.6±0.1)	0.73 (0.71±0.02)	0.68 (0.69±0.01)	7.7 (7.6±0.1)
YD2-*o*-C8	17.3 (17.4±0.1)	0.78 (0.77±0.01)	0.65 (0.65±0.02)	8.8 (8.7±0.1)

[a] Values represent photovoltaic parameters exhibiting the highest η value. Values in parenthesis also denote average values from five independent experiments.

We applied electrical impedance spectroscopy (EIS) to rationalize the difference in V_{OC}. The EIS Nyquist plots were obtained under standard AM 1.5 illumination at open-circuit conditions (Figure S15). The middle semicircle corresponds to the electron transfer process at the TiO_2-dye-electrolyte interface (R_p). A small R_p implies small charge recombination resistance between the TiO_2 and the electrolyte. In fact, a R_p value of the DSSC based on **YD2-*o*-C8T** (22.0 Ω) is smaller than that based on **YD2-*o*-C8** (28.7 Ω), which is consistent with the slightly lower V_{OC} value for **YD2-*o*-C8T**.

Finally, we investigated the long-term durability of DSSCs based on **YD2-*o*-C8T** and **YD2-*o*-C8**. The porphyrin-stained TiO_2 films were immersed into a 1:1 mixture of THF/H_2O with 28 mM acetic acid or 1 mM NaOH. Then, the amount of the dye on TiO_2 as a function of immersion time was determined from absorbance of the TiO_2 film (Figure 4a). Although **YD2-*o*-C8** completely dissociated from the TiO_2 surface within 1 hour under both acidic and basic conditions, more than 95% of **YD2-*o*-C8T** were retained in 8 hours. This result unambiguously corroborates that tropolone is a robust anchoring group compared to benzoic acid. Furthermore, the long-term durability of the DSSCs based on **YD2-*o*-C8T** and **YD2-*o*-C8** were assessed under continuous white light illumination (100 mW cm^{-2} at 25ºC, Figure 4b). The **YD2-*o*-C8T** and **YD2-*o*-C8** cells show 13% and 33% decrease in 500 h, which strongly supports the advantage of the tropolone anchoring group in terms of long-term durability of DSSCs. To the best of our knowledge, this is the first quantitative comparison of the long-term durability of DSSCs in terms of the difference in anchoring groups.

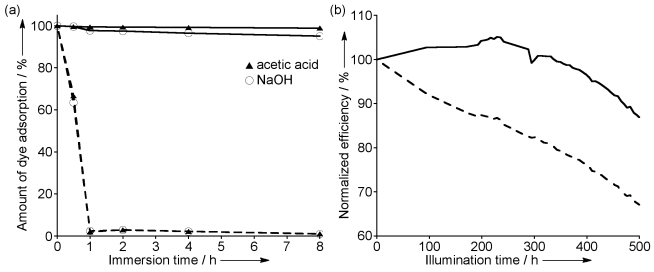

Figure 4. (a) Plots of the amount of porphyrin on the TiO_2 surface as a function of immersion time for **YD2-*o*-C8T** (solid line) and **YD2-*o*-C8** (dashed line) and (b) plots of the normalized η-value (average of two independent experiments) as a function of illumination time for DSSCs based on **YD2-*o*-C8T** (solid line) and **YD2-*o*-C8** (dashed line).

In summary, we have employed tropolone for the first time as the anchoring group of DSSCs. The DSSC based on **YD2-*o*-C8T** with tropolone exhibited the power conversion efficiency of 7.7%, which is almost comparable to that based on **YD2-*o*-C8** with benzoic acid as the anchoring group. More importantly, **YD2-*o*-C8T** was found to display the superior DSSC durability as well as binding ability to TiO_2 to **YD2-*o*-C8**. We believe that tropolone is the highly attractive anchoring group that is applicable to any kind of dye for DSSCs that would realize the high device durability as well as excellent photovoltaic performance.

Acknowledgements

The work was supported by Advanced Low Carbon Technology Research and Development Program (ALCA) from JST and Grants-in-Aid (No.25220801 to H.I.) from MEXT, Japan.

Keywords: sensitizer • tropolone • solar cell • porphyrin • anchoring group

[1] B. O'Regan, M. Grätzel, *Nature* **1991**, *353*, 737–740.

[2] a) M. K. Nazeeruddin, F. De Angelis, S. Fantacci, A. Selloni, G. Viscardi, P. Liska, S. Ito, B. Takeru, M. Grätzel, *J. Am. Chem. Soc.* **2005**, *127*, 16835–16847; b) F. Gao, Y. Wang, D. Shi, J. Zhang, M. Wang, X. Jing, R. Humphry-Baker, P. Wang, S. M. Zakeeruddin, M. Grätzel, *J. Am. Chem. Soc.* **2008**, *130*, 10720–10728; c) C. Chen, M. Wang, J. Li, N. Pootrakulchote, L. Alibabaei, C.-h. Ngoc-le, J. Decoppet, J. Tsai, C. Grätzel, C. Wu, S. M. Zakeeruddin, M. Grätzel, *ACS Nano* **2009**, *3*, 3103–3109; d) L. Han, A. Islam, H. Chen, C. Malapaka, B. Chiranjeevi, S. Zhang, X. Yang, M. Yanagida, *Energy Environ. Sci.* **2012**, *5*, 6057–6060.

[3] a) Y. Ooyama, Y. Harima, *Eur. J. Org. Chem.* **2009**, 2903–2934; b) A. Mishra, M. K. R. Fischer, P. Bäuerle, *Angew. Chem.* **2009**, *121*, 2510–2536; *Angew. Chem. Int. Ed.* **2009**, *48*, 2474–2499; c) W. Zeng, Y. Cao, Y. Bai, Y. Wang, Y. Shi, M. Zhang, F. Wang, C. Pan, P. Wang, *Chem. Mater.* **2010**, *22*, 1915–1925; d) M. Zhang, Y. Wang, M. Xu, W. Ma, R. Li, P. Wang, *Energy Environ. Sci.* **2013**, *6*, 2944–2949; e) K. Kakiage, Y. Aoyama, T. Yano, T. Otsuka, T. Kyomen, M. Unno, M. Hanaya, *Chem. Commun.* **2014**, *50*, 6379–6381.

[4] a) H. Imahori, T. Umeyama, S. Ito, *Acc. Chem. Res.* **2009**, *42*, 1809–1818; b) M. V. Martínez-Díaz, G. de la Torre, T. Torres, *Chem. Commun.* **2010**, *46*, 7090–7108; c) L.-L. Li, E. W.-G. Diau, *Chem. Soc. Rev.* **2013**, *42*, 291–304; d) M. Urbani, M. Grätzel, M. K. Nazeeruddin, T. Torres, *Chem. Rev.* **2014**, *114*, 12330–12396; e) K. Ladomenou, T. N. Kitsopoulos, G. D. Sharma, A. G. Coutsolelos, *RSC Adv.* **2014**, *4*, 21379–21404; f) T. Higashino, H. Imahori, *Dalton Trans.* **2015**, *44*, 448–463.

[5] a) T. Bessho, S. M. Zakeeruddin, C.-Y. Yeh, E. W.-G. Diau, M. Grätzel, *Angew. Chem.* **2010**, *122*, 6796–6799; *Angew. Chem. Int. Ed.* **2010**, *49*, 6646–6649; b) A. Yella, H.-W. Lee, H. N. Tsao, C. Yi, A. K. Chandiran, M. K. Nazeeruddin, E. W.-G. Diau, C.-Y. Yeh, S. M. Zakeeruddin, M. Grätzel, *Science* **2011**, *334*, 629–34; c) K. Kurotobi, Y. Toude, K. Kawamoto, Y. Fujimori, S. Ito, P. Chabera, V. Sundström, H. Imahori, *Chem. Eur. J.* **2013**, *19*, 17075–17081; d) A. Yella, C.-L. Mai, S. M. Zakeeruddin, S.-N. Chang, C.-H. Hsieh, C.-Y. Yeh, M. Grätzel, *Angew. Chem.* **2014**, *126*, 3017–3021; *Angew. Chem. Int. Ed.* **2014**, *53*, 2973–2977; e) S. Mathew, A. Yella, P. Gao, R. Humphry-Baker, B. F. E. Curchod, N. Ashari-Astani, I. Tavernelli, U. Rothlisberger, M. K. Nazeeruddin, M. Grätzel, *Nature Chem.* **2014**, *6*, 242–247; f) J. Luo, M. Xu, R. Li, K.-W. Huang, C. Jiang, Q. Qi, W. Zeng, J. Zhang, C. Chi, P. Wang, J. Wu, *J. Am. Chem. Soc.* **2014**, *136*, 265–272.

[6] M. I. Asghar, K. Miettunen, J. Halme, P. Vahermaa, M. Toivola, K. Aitola, P. Lund, *Energy Environ. Sci.* **2010**, *3*, 418–426.

[7] a) H. He, A. Gurung, L. Si, *Chem. Commun.* **2012**, *48*, 5910–5912; b) L. Si, H. He, K. Zhu, *New J. Chem.* **2014**, *38*, 1565–1572.

[8] a) T. Asao, Y. Kikuchi, *Chem. Lett.* **1972**, *1*, 413–416; b) M. C. Barret, M. F. Mahon, K. C. Molloy, J. W. Steed, P. Wrightt, *Inorg. Chem.* **2001**, *40*, 4384–4388; c) K. Nomiya, K. Onodera, K. Tsukagoshi, K. Shimada, A. Yoshizawa, T. A. Itoyanagi, A. Sugie, S. Tsuruta, R. Sato, N. C. Kasuga, *Inorg. Chim. Acta* **2009**, *362*, 43–55.

[9] a) Y. Sakata, S. Hiraoka, M. Shionoya, *Chem. Eur. J.* **2010**, *16*, 3318–3325; b) H. Otani, C. Sumi, H. Shimizu, M. Hasegawa, M. Iyoda, *Chem. Lett.* **2014**, *43*, 1710–1712.

[10] a) J. R. Chipperfield, S. Clark, J. Elliott, E. Sinn, *Chem. Commun.* **1998**, 195–196; b) J. M. Elliott, J. R. Chipperfield, S. Clark, S. J. Teat, E. Sinn, *Inorg. Chem.* **2002**, *41*, 293–299; c) A. Mori, R. Mori, M. Takemoto, S. Yamamoto, D. Kuribayashi, K. Uno, K. Kubo, S. Ujiie, *J. Mater. Chem.* **2005**, *15*, 3005–3014.

[11] J. Potenziano, R. Spitale, M. E. Janik, *Synth. Commun.* **2005**, *35*, 2005–2016.

[12] M. J. Frisch, *et al*., *Gaussian 09*, revision D.01; Gaussian, Inc.; Wallingford, CT, **2013**.

[13] a) H. P. Koch, *J. Chem. Soc.* **1951**, 512–515; b) Y. Ikegami, *Bull. Chem. Soc. Jpn.* **1961**, *34*, 94–98.

[14] a) K. Wagner, M. J. Griffith, M. James, A. J. Mozer, P. Wagner, G. Triani, D. L. Officer, G. G. Wallace, *J. Phys. Chem. C* **2011**, *115*, 317–326; b) M. J. Griffith, K. Sunahara, A. Furube, A. J. Mozer, D. L. Officer, P. Wagner, G. G. Wallace, S. Mori, *J. Phys. Chem. C* **2013**, *117*, 11885–11898.

[15] a) B. J. Brennan, M. J. Llansola Portolés, P. A. Liddell, T. A. Moore, A. L. Moore, D. Gust, *Phys. Chem. Chem. Phys.* **2013**, *15*, 16605–16614; b) D. Daphnomili, G. D. Sharma, S. Biswas, K. R. Justin Thomas, A. G. Coutsolelos, *J. Photochem. Photobiol. A Chem.* **2013**, *253*, 88–96; c) F. Gou, X. Jiang, R. Fang, H. Jing, Z. Zhu, *ACS Appl. Mater. Interfaces* **2014**, *6*, 6697–6703.

Tropolone has been employed for the first time as an anchoring group for dye-sensitized solar cells (DSSCs). The DSSC based on a porphyrin with the tropolone moiety exhibited the comparable power conversion efficiency as well as superior DSSC durability to a reference porphyrin with a carboxylic group. Tropolone is the highly promising anchoring group of any dyes for high-performance robust DSSCs.

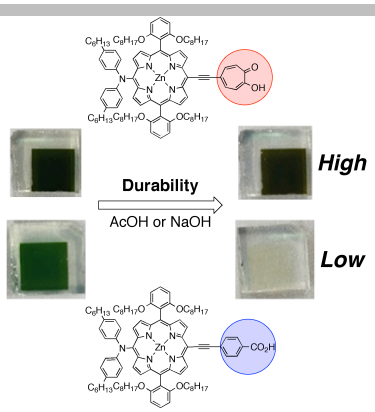

*T. Higashino, Y. Fujimori, K. Sugiura, Y. Tsuji, S. Ito, H. Imahori**

Tropolone as High-Performance Robust Anchoring Group for Dye-Sensitized Solar Cells

Supplementary Information

Tropolone as High-Performance Robust Anchoring Group for Dye-Sensitized Solar Cells

Tomohiro Higashino, Yamato Fujimori, Kenichi Sugiura, Yukihiro Tsuji, Seigo Ito, Hiroshi Imahori*

Department of Molecular Engineering, Graduate School of Engineering, Kyoto University, Nishikyo-ku, Kyoto 615-8510, Japan

Graduate School of Engineering, University of Hyogo, 2167 Shosha, Himeji, Hyogo 671-2280, Japan

Institute for Integrated Cell-Material Sciences (WPI-iCeMS), Kyoto University, Nishikyo-ku, Kyoto 615-8510, Japan

E-mail: imahori@scl.kyoto-u.ac.jp

Contents

1. Experimental Section

Instrumentation and Materials.

Commercially available solvents and reagents were used without further purification unless otherwise mentioned. Silica-gel column chromatography was performed with UltraPure Silica Gel (230-400 mesh, SiliCycle) unless otherwise noted. Thin-layer chromatography (TLC) was performed with Silica gel 60 F_{254} (Merck). UV/Vis/NIR absorption spectra of solutions and films were measured with a Perkin-Elmer Lambda 900 UV/vis/NIR spectrometer. Steady-state fluorescence spectra were obtained by a HORIBA Nanolog spectrometer. ^{1}H and ^{13}C NMR spectra were recorded with a JEOL EX-400 spectrometer (operating at 400 MHz for ^{1}H and 100 MHz for ^{13}C) by using the residual solvent as the internal reference for ^{1}H ($CDCl_3$: δ = 7.26 ppm) and ^{13}C ($CDCl_3$: δ = 77.16 ppm). High-resolution mass spectra (HRMS) were measured on a Thermo Fischer Scientific EXACTIVE spectrometer for ESI measurements. Attenuated total reflectance-Fourier transform infrared (ATR-FTIR) spectra were taken with the golden gate diamond anvil ATR accessory (NICOLET 6700, Thermo scientific), using typically 64 scans at a resolution of 2 cm^{-1}. All samples were placed in contact with the diamond window using the same mechanical force. Electrical impedance spectra were measured on SP-150 (Bio-Logic) spectrometer.

Electrochemical Measurements.

Electrochemical measurements were made using an ALS 630a electrochemical analyzer. Redox potentials were determined by differential pulse voltammetry (DPV) in THF containing 0.1 M tetrabutylammonium hexafluorophosphate (Bu_4NPF_6). A glassy carbon (3 mm diameter) working electrode, $Ag/AgNO_3$ reference electrode, and Pt wire counter electrode were employed. Ferrocene (+0.642 V vs NHE) was used as an internal standard for the DPV measurements.

Density Functional Theory (DFT) Calculations.

All calculations were carried out using the *Gaussian 09* program.[S1] All structures of porphyrins were fully optimized without any symmetry restriction. The calculations were performed by the density functional theory (DFT) method with restricted B3LYP (Becke's three-parameter hybrid exchange functionals and the Lee-Yang-Parr correlation functional) level, employing a basis set 6-31G(d) for C, H, N, O and Zn.

X-Ray Photoelectron Spectroscopy (XPS) Measurements.

The XPS data were acquired using an ULVAC-PHI 5500MT system equipped with Mg Kα X-ray source (1253.6 eV) and a hemispherical energy analyzer. Samples were mounted on indium foil

and then transferred to an analyzer chamber. The electron takeoff angle was set at 45°. The pressure of the main XPS chamber was maintained at less than 1×10^{-8} Torr during analysis. Peaks of interests were deconvoluted by Gaussian/Lorentzian mixed functions with PeakFit 4.12 program. All the samples for XPS measurements were made by the same method for preparing the porphyrin on the TiO_2 electrodes (vide infra).

Preparation of Porphyrin-Sensitized TiO_2 Electrode and Photovoltaic Measurements.

The preparation of TiO_2 electrodes and the fabrication of the sealed cells for photovoltaic measurements were performed according to literature.[S2,S3] We used two types of TiO_2 pastes, one composed of nanocrystalline TiO_2 particles (20 nm, CCIC:PST23NR, JGC-CCIC) and another containing submicrocrystalline TiO_2 particles (400 nm, CCIC:PST400C, JGC-CCIC), to form the transparent and the light-scattering layers of the photoanode, respectively. To prepare the working electrodes, FTO glasses (solar 4mm thickness, 10 Ω/□, Nippon Sheet Glass) were first cleaned in a detergent solution using an ultrasonic bath for 10 min and then rinsed with distilled water and ethanol. After UV-O_3 irradiation for 18 min, the FTO glass plates were immersed into a 40 mM aqueous $TiCl_4$ solution at 70 °C for 30 min and washed with distilled water and ethanol. A layer of the nanocrystalline TiO_2 paste was coated on the FTO glass plate by a screen-printing method, kept in a clean box for a few minutes, and then dried over 6 min at 125 °C. This screen-printing procedure with the nanocrystalline TiO_2 paste was repeated to reach a thickness of 12 μm. After drying the films at 125 °C, a layer of the submicrocrystalline TiO_2 paste was further deposited by screen-printing in the same method as the fabrication of the nanocrystalline TiO_2 layer, resulting in formation of a light-scattering TiO_2 film of 4 μm on the transparent TiO_2 film of 12 μm. Finally, the electrodes coated with the TiO_2 pastes were gradually heated under an airflow at 325 °C for 5 min, at 375 °C for 5 min, at 450 °C for 15 min, and at 500 °C for 15 min. The thickness of the films was determined using a surface profiler (SURFCOM 130A, ACCRETECH). The size of the TiO_2 film was 0.16 cm^2 (4 × 4 mm). The TiO_2 electrode was treated again with 40 mM $TiCl_4$ solution at 70 °C for 30 min and then rinsed with distilled water and ethanol, sintered at 500 °C for 30 min, and cooled to 70 °C before dipping into the dye solution. The TiO_2 electrode was immersed into an ethanol/toluene (v/v=1/1) solution of the porphyrins (0.20 mM) in the presence or absence of chenodeoxycholic acid (CDCA) at 25 °C. The porphyrin surface coverage adsorbed on the TiO_2 films (Γ, mol cm^{-2}) was determined by measuring the absorbance of the porphyrin solution that was dissolved from porphyrin-stained TiO_2 film into 0.1 M NaOH solution of 1:1 mixture of THF and water.

The counter electrode was prepared by drilling a small hole in an FTO glass (solar 1 mm thickness, 10 Ω/□, Nippon Sheet Glass), rinsing with distilled water and ethanol followed by treatment with 0.1 M HCl solution in 2-propanol using an ultrasonic bath for 15 min. After heating in air for 15 min at 400 °C, the platinum was deposited on the FTO glass by coating with a drop of H_2PtCl_6 solution (2 mg in 1 mL of ethanol) twice. Finally, the FTO glass was heated at 400 °C for 15 min to obtain the counter Pt-electrode.

A sandwich cell was prepared by using the dye-anchored TiO_2 film as a working electrode and a counter Pt-electrode, which were assembled with a hotmelt-ionomer film Surlyn polymer gasket (DuPont, 50 μm), and the superimposed electrodes were tightly held and heated at 110 °C to seal the two electrodes. The aperture of the Surlyn frame was 2 mm larger than that of the area of the TiO_2 film, and its width was 1 mm. The hole in the counter Pt-electrode was sealed by a film of Surlyn. A hole was then made in the film of Surlyn covering the hole with a needle. A drop of an electrolyte was put on the hole in the back of the counter Pt-electrode. It was introduced into the cell via vacuum backfilling. Finally, the hole was sealed using Surlyn film and a cover glass (0.13–0.17 mm thickness). A solder was applied on each edge of the FTO electrodes. The electrolyte solution used was 1.0 M 1,3-dimethylimidazolium iodide, 0.03 M I_2, 0.05 M LiI, 0.1 M guanidinium thiocyanate and 0.50 M 4-*tert*-butylpyridine in 85:15 mixture of acetonitrile and valeronitrile.

Incident photon-to-current efficiency (IPCE) and photocurrent-voltage (*I-V*) performance were measured on an action spectrum measurement setup (CEP-2000RR, BUNKOUKEIKI) and a solar simulator (PEC-L10, Peccell Technologies) with a simulated sunlight of AM 1.5 (100 mW cm^{-2}), respectively: IPCE (%) = 100 × 1240 × $i/(W_{in} \times \lambda)$, where i is the photocurrent density (A cm^{-2}) W_{in} is the incident light intensity (W cm^{-2}), and λ is the excitation wavelength (nm). During the photovoltaic measurements, a black plastic tape was attached on the back of the TiO_2 electrode except for the TiO_2 film region to reduce scattering light. The convolution of the spectral response in the photocurrent action spectrum with the photon flux of the AM 1.5G spectrum provided the estimated J_{SC}-value, which is in good agreement with the J_{SC}-value obtained from the *I-V* performance.

2. Synthesis

[5-Bis(4-hexylphenyl)amino-15-(Triisopropylsilyl)ethynyl-10,20-bis(2,6-di-octyloxyphenyl)porphyrinato]zinc(II) (**1**),[S4] 5-iodo-2-methoxytropone,[S5] and **YD2-*o*-C8**[S4] were prepared according to literature.

{5,15-Bis(2,6-dioctyloxyphenyl)-10-bis(4-hexylphenyl)amino-20-[(2-methoxytropon-5-yl)ethynyl]porphyrinato}zinc(II) (2): To a stirred solution of **1** (80 mg, 0.051 mmol) in dry THF (6.7 mL), TBAF (0.26 mL, 1 M in THF) was added. After 30 min, the reaction was quenched with H_2O and the reaction mixture was diluted with CH_2Cl_2. Layers were separated and organic layer was dried over Na_2SO_4 and concentrated. A solution of the residue, 5-iodo-2-methoxytropone (65 mg, 0.25 mmol), $Pd_2(dba)_3$ (14 mg, 0.015 mmol), triphenylarsine (31 mg, 0.10 mmol) and NEt_3 (2.3 mL) in dry THF (12 mL) was freeze-pump-thaw degassed and stirred at 80 ºC overnight. The reaction mixture was cooled to room temperature and concentrated. The crude mixture was purified by silica-gel column chromatography (1:1 hexane-EtOAc) to give **2** (71 mg, 0.046 mmol, 90% yield) as a green solid.

^{1}H NMR (400 MHz; $CDCl_3$): δ = 9.57 (d, J = 4.4 Hz, 2H), 9.17 (d, J = 4.8 Hz, 2H), 8.88 (d, J = 4.4 Hz, 2H), 8.68 (d, J = 4.4 Hz, 2H), 7.91 (d, J = 12.8 Hz, 1H), 7.83 (d, J = 10.4 Hz, 1H), 7.66 (t, J = 8.0 Hz, 2H), 7.40 (d, J = 12.8 Hz, 1H), 7.20 (d, J = 8.8 Hz, 4H), 6.90-6.97 (m, 9H), 4.06 (s, 3H), 3.83 (t, J = 6.4 Hz, 8H), 2.46 (t, J = 8.0 Hz, 4H), 1.23-1.29 (m, 16H), 0.95-1.02 (m, 8H), 0.77-0.90 (m, 16H), 0.44-0.69 (m, 42H) ppm. ^{13}C NMR (100 MHz; $CDCl_3$): δ = 180.02, 164.78, 159.78, 152.06, 151.81, 150.42, 150.34, 139.05, 136.61, 134.88, 134.70, 132.28, 132.17, 130.66, 129.86, 129.82, 128.69, 125.28, 123.56, 121.97, 120.51, 114.80, 112.54, 105.07, 97.68, 96.85, 96.49, 68.52, 56.59, 35.23, 31.72, 31.51, 31.37, 29.69, 29.10, 28.61, 28.56, 28.43, 25.12, 22.59, 22.25, 14.07, 13.81 ppm. HR-MS (ESI-MS) m/z calcd. for $C_{98}H_{123}ClN_5O_6Zn[M+Cl]^-$: 1564.8459, found 1564.8451. FT-IR (ATR) ν_{max}: 2921, 2851, 2174, 1624, 1577, 1504, 1453, 1403, 1377, 1337, 1298, 1274, 1244, 1205, 1171, 1095, 1059, 995, 939, 848, 824, 791, 768, 710, 653, 628 cm^{-1}. mp >300ºC.

{5,15-Bis(2,6-dioctyloxyphenyl)-10-bis(4-hexylphenyl)amino-20-[(tropolon-5-yl)ethynyl]porphyrinato}zinc(II) (YD2-*o*-C8T): To a solution of **2** (62 mg, 0.040 mmol) in THF (50 mL), ethanol (25 mL), and H_2O (25 mL), KOH (435 mg, 7.8 mmol) was added and the mixture was refluxed for 3h. The reaction mixture was cooled to room temperature and quenched with aqueous saturated NH_4Cl. Layers were separated and organic layer was dried over Na_2SO_4 and concentrated. The

crude mixture was purified by reprecipitation from CH_2Cl_2/acetonitrile to give **YD2-*o*-C8T** (36 mg, 0.016 mmol, 42% yield) as a green solid.

^{1}H NMR (400 MHz; $CDCl_3$): δ = 9.57 (d, J = 4.4 Hz, 2H), 9.17 (d, J = 4.4 Hz, 2H), 8.88 (d, J = 4.8 Hz, 2H), 8.68 (d, J = 4.8 Hz, 2H), 8.11 (d, J = 11.6 Hz, 2H), 7.66 (t, J = 8.4 Hz, 2H), 7.50 (d, J = 11.6 Hz, 2H), 7.20 (d, J = 8.4 Hz, 4H), 6.92-6.97 (m, 8H), 3.83 (t, J = 6.4 Hz, 8H), 2.45 (t, J = 8.0 Hz, 4H), 1.23-1.29 (m, 16H), 0.96-1.02 (m, 8H), 0.77-0.84 (m, 16H), 0.45-0.64 (m, 42H) ppm. ^{13}C NMR (400 MHz; $CDCl_3$): δ = 170.98, 159.80, 152.05, 151.82, 150.44, 150.42, 150.36, 139.93, 134.69, 132.32, 132.13, 130.66, 129.85, 129.75, 128.69, 125.98, 123.88, 123.62, 121.97, 120.56, 114.80, 105.08, 97.42, 97.04, 96.93, 68.54, 35.24, 31.72, 31.38, 29.11, 28.62, 28.57, 28.44, 25.12, 22.59, 22.25, 14.07, 13.81 ppm. HR-MS (ESI-MS) m/z calcd. for $C_{97}H_{121}N_5O_6Zn[M]^+$: 1515.8618, found 1515.8618. UV/vis (THF) λ_{max} ($\varepsilon/10^3$ M^{-1} cm^{-1}): 465 (169), 583 (11.0), 656 (42.3) nm. FT-IR (ATR) ν_{max}: 3271, 2922, 2852, 2173, 1585, 1540, 1506, 1454, 1376, 1337, 1298, 1245, 1204, 1095, 1048, 995, 972, 941, 879, 849, 824, 792, 768, 711, 654, 615 cm^{-1}. mp >300°C.

3. High-Resolution ESI-MS

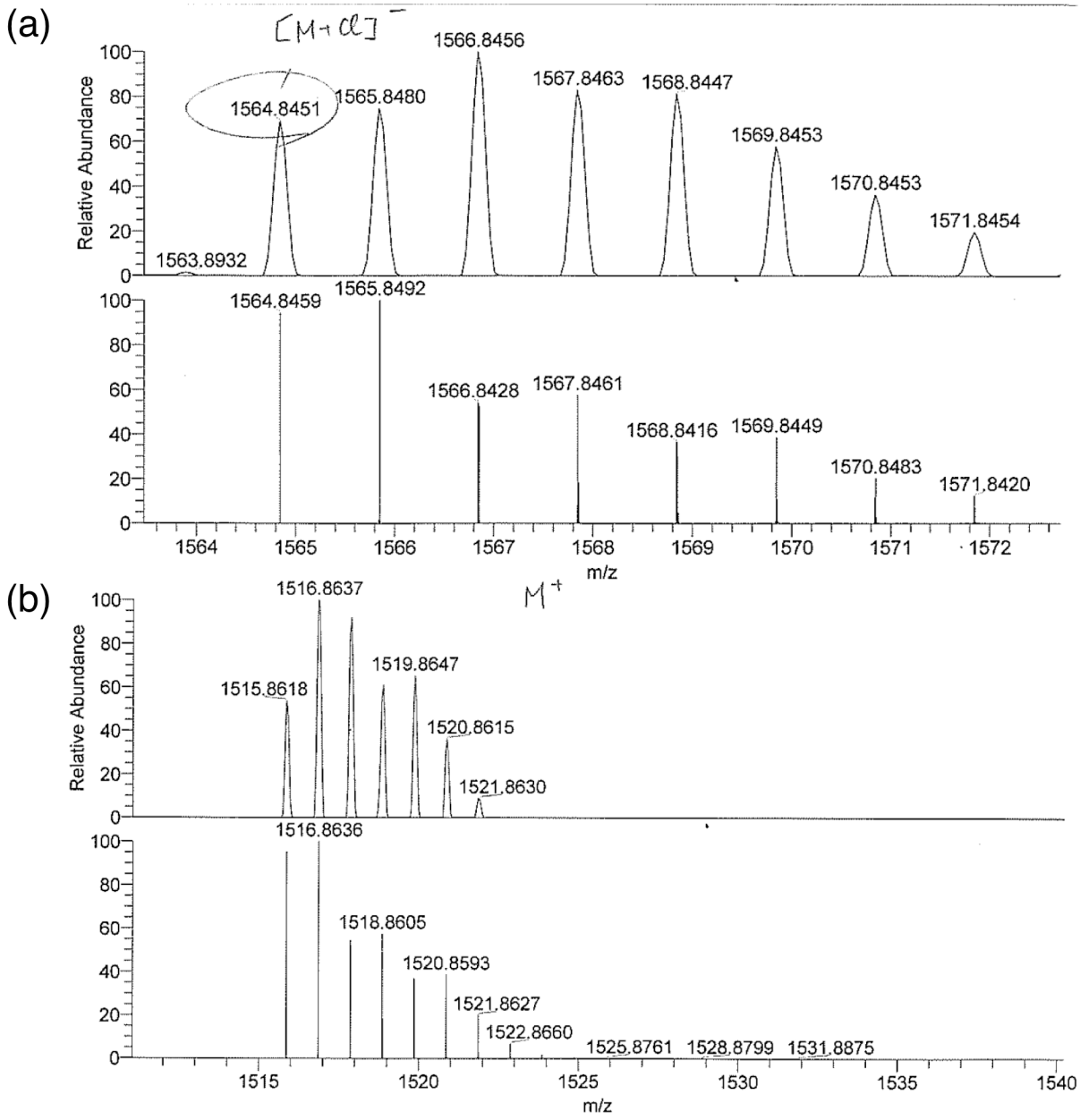

Figure S1. Observed (top) and simulated (bottom) high-resolution ESI-MS of (a) **2** and (b) **YD2-*o*-C8T**.

4. NMR Spectra

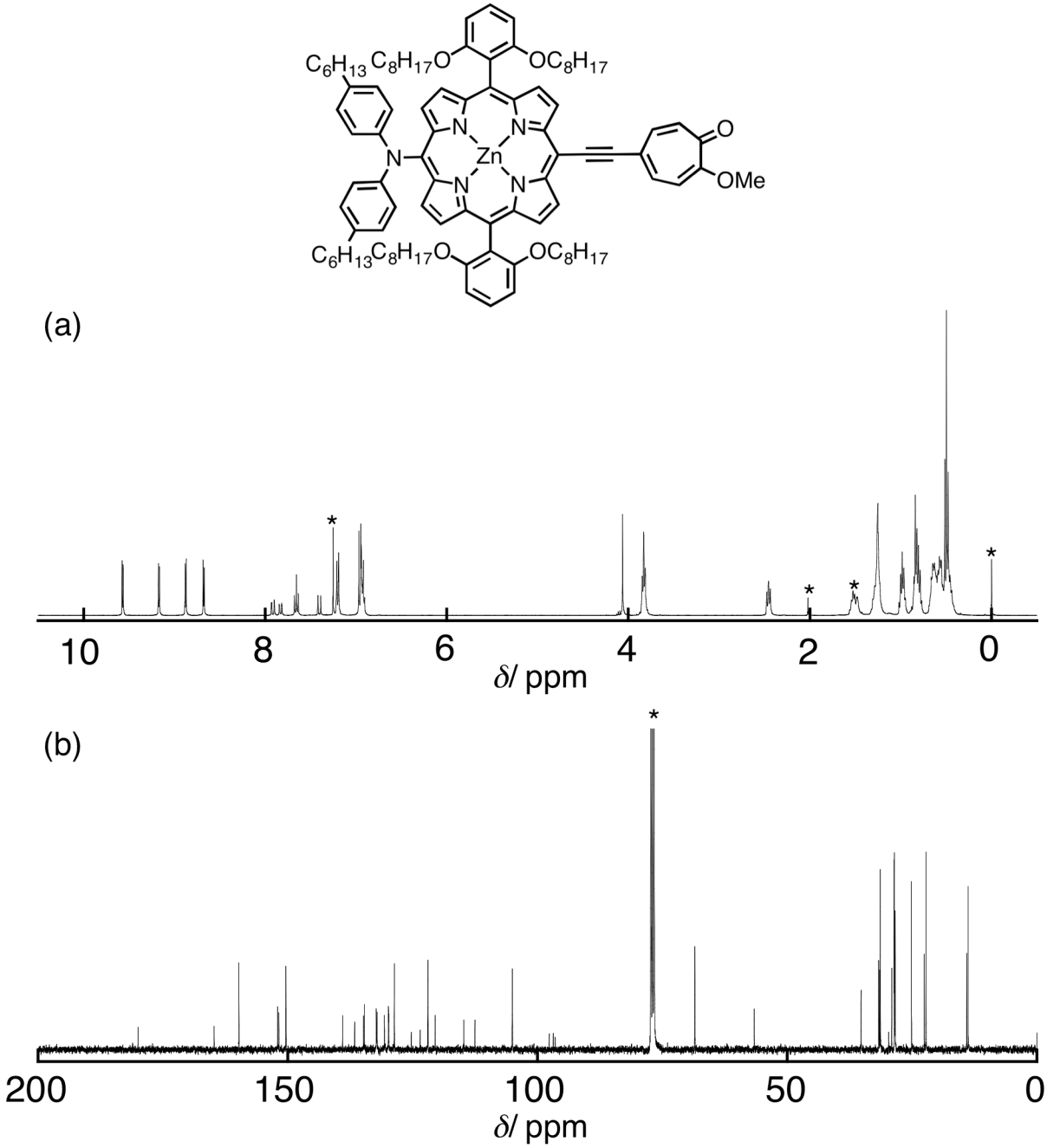

Figure S2. (a) ^{1}H and (b) ^{13}C NMR spectra of **2** at 25 °C in $CDCl_3$. Peaks marked with * are attributable to residual solvents.

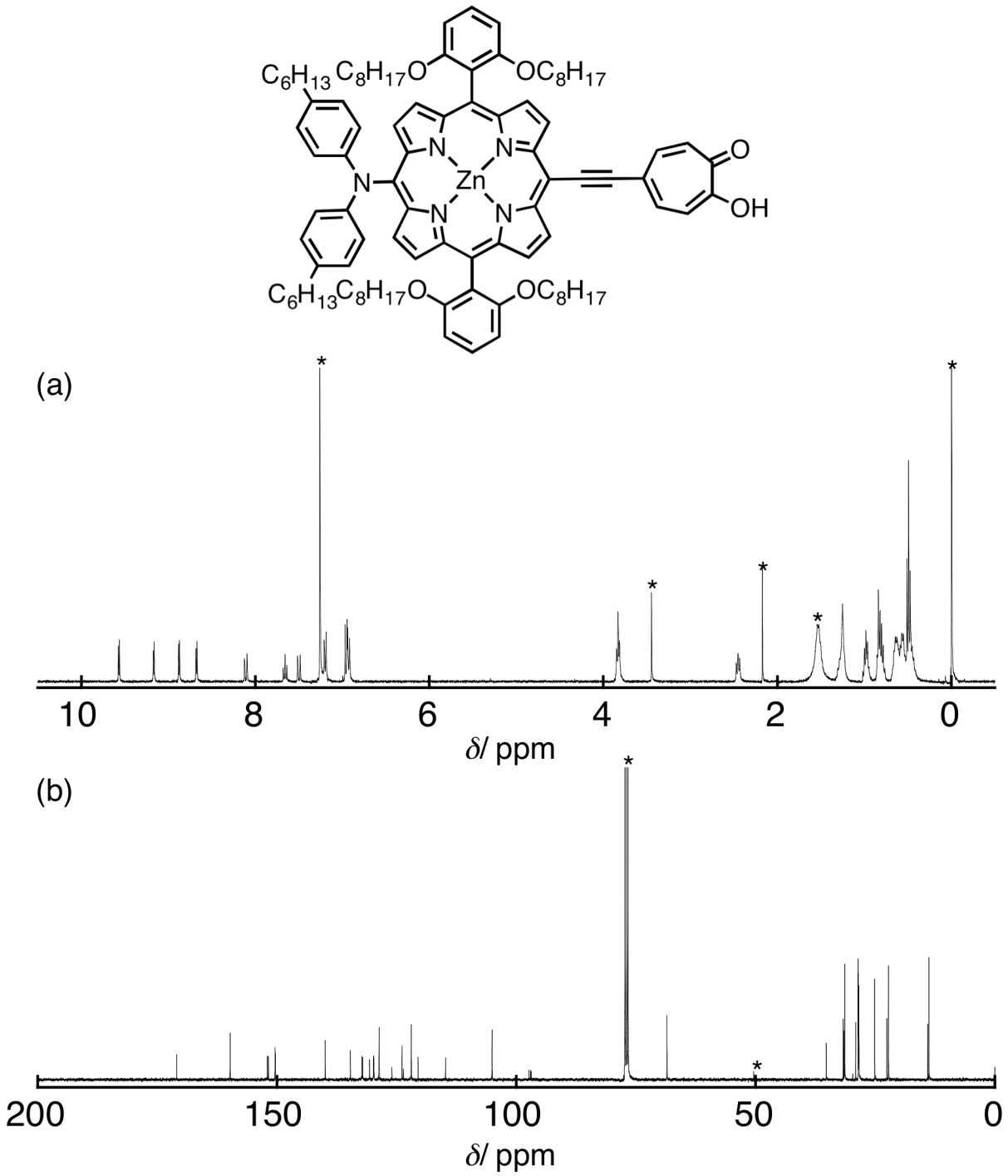

Figure S3. (a) ^{1}H and (b) ^{13}C NMR spectra of **YD2-*o*-C8T** at 25 °C in $CDCl_3$. Peaks marked with * are attributable to residual solvents.

5. Fluorescence Spectra

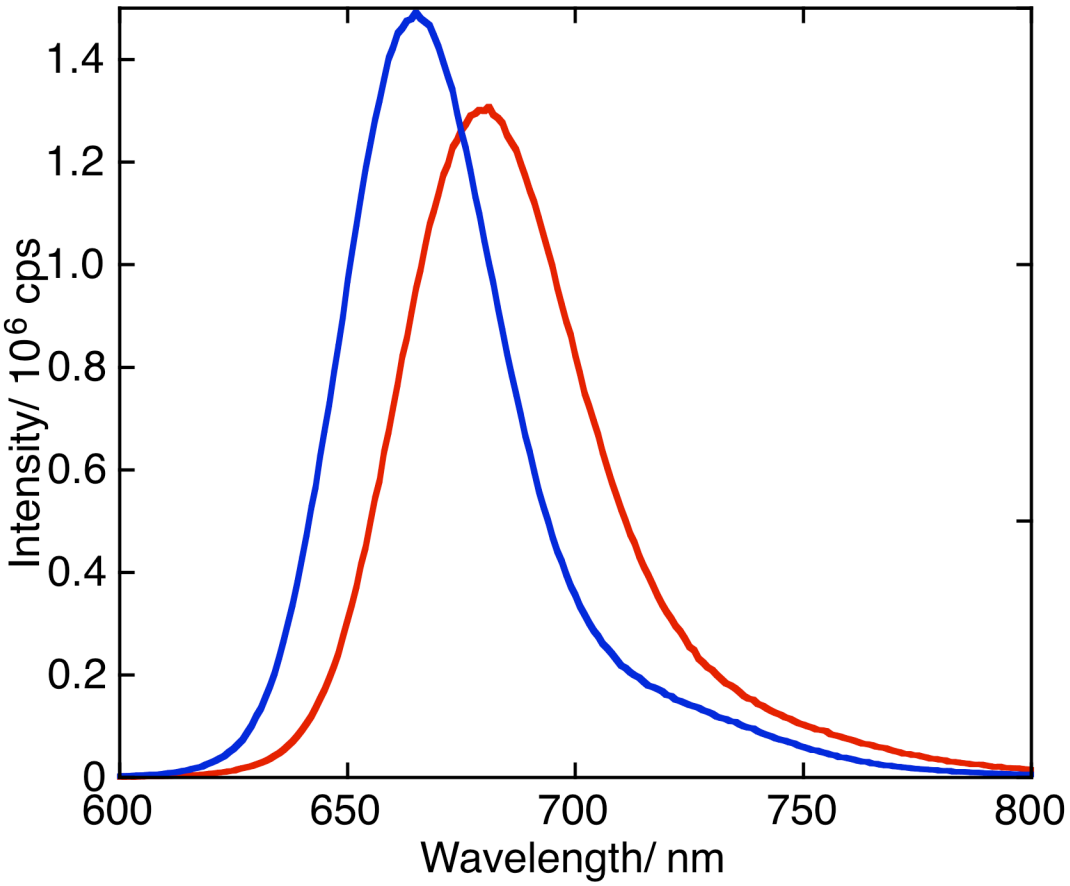

Figure S4. Fluorescence spectra of **YD2-*o*-C8T** (red) and **YD2-*o*-C8** (blue) in THF. The samples were excited at Soret band peak where the absorbance was adjusted to be identical for comparison.

6. DPV Curves

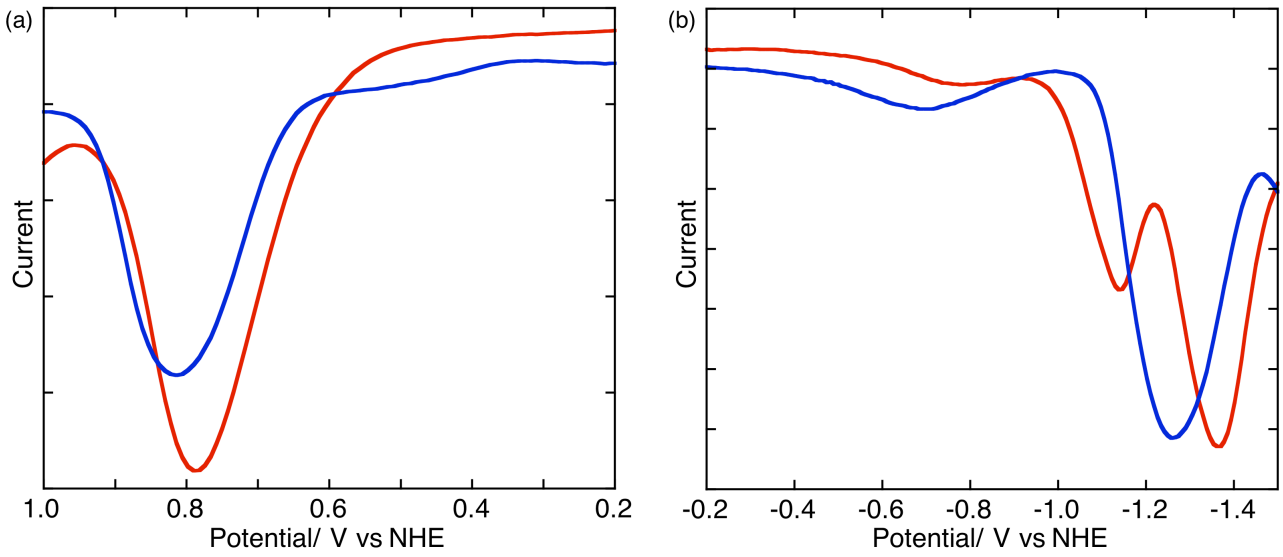

Figure S5. Differential pulse voltammetry (DPV) curves of **YD2-*o*-C8T** (red) and **YD2-*o*-C8** (blue). The sweeps are shown in (a) oxidation and (b) reduction regions with a sweep rate of 40 mV s^{-1}.

7. Molecular Orbital Diagrams

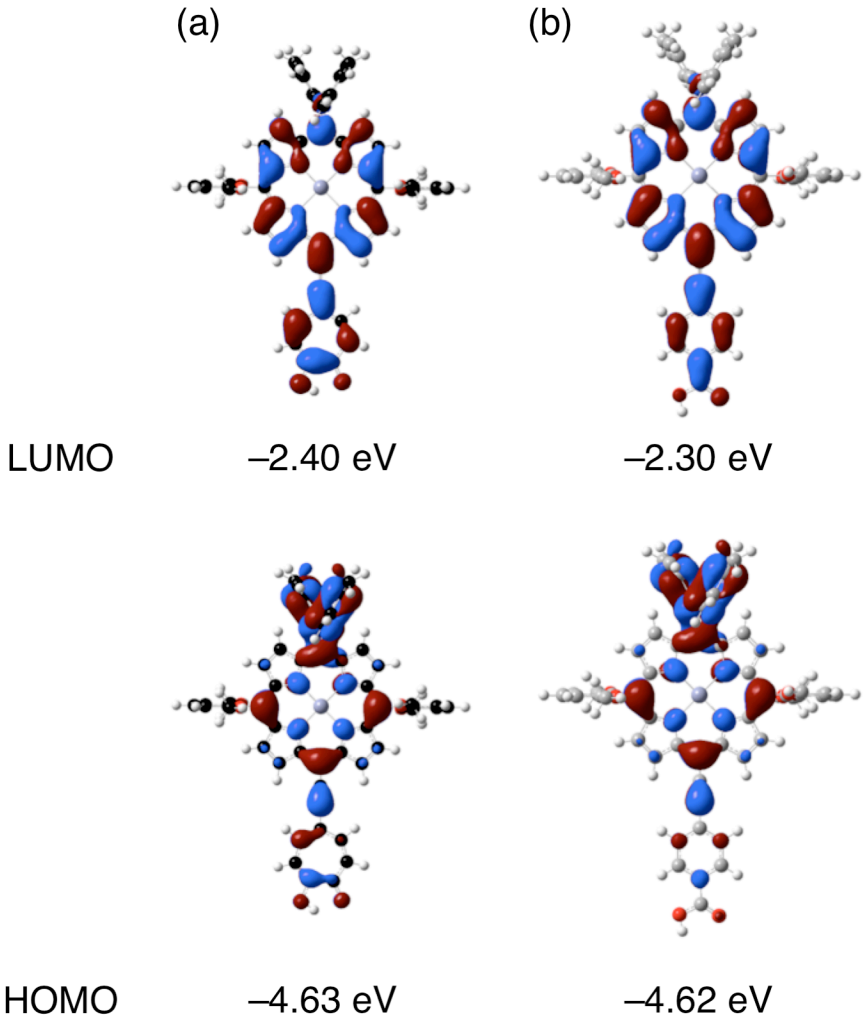

Figure S6. Selected molecular orbital diagrams for (a) **YD2-*o*-C8T** and (b) **YD2-*o*-C8** obtained by DFT calculations with B3LYP/6-31G(d). To simplify the calculations, alkyl chains on the diarylamino groups were replaced with methyl ones, whereas octyloxy groups on the phenyl groups were replaced with methoxy ones.

8. Adsorption behavior on TiO_2

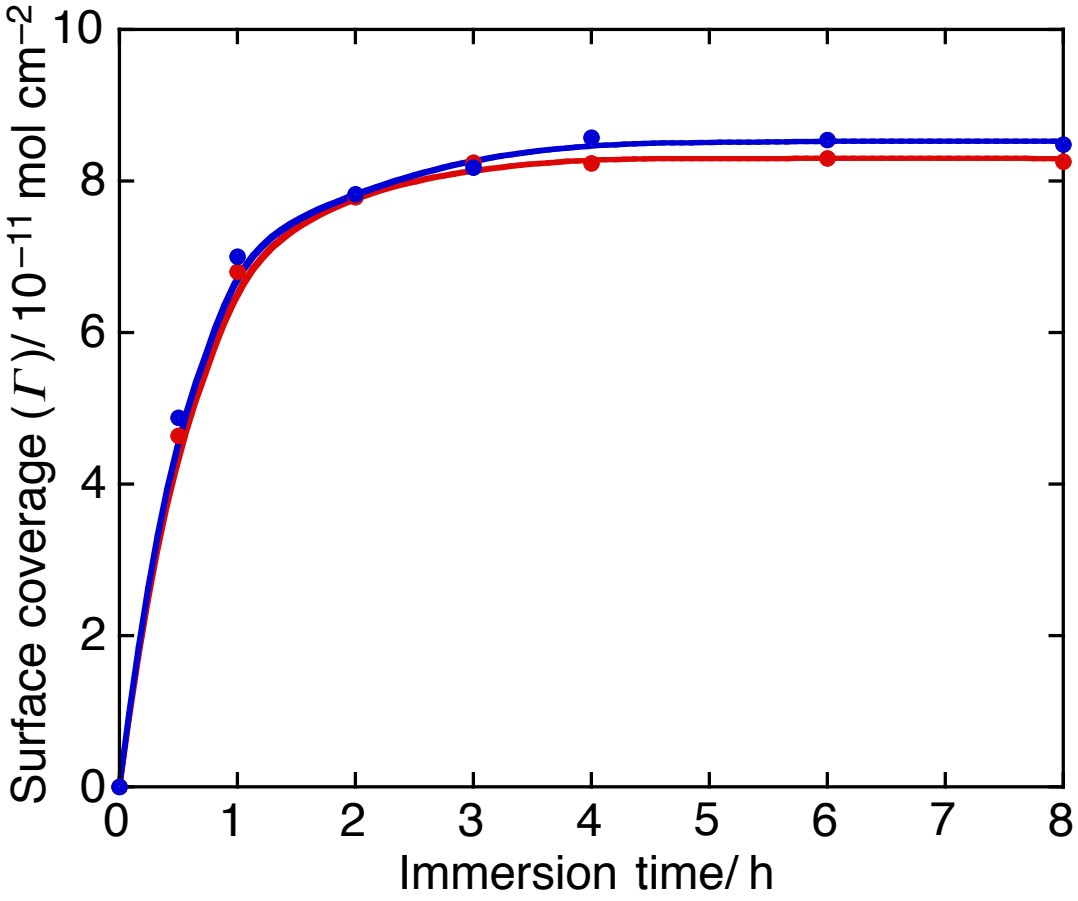

Figure S7. Plots of porphyrin surface coverage (Γ) as a function of immersion time for **YD2-*o*-C8T** (red) and **YD2-*o*-C8** (blue) that adsorb on the TiO_2 films without the scattering layer.

9. FT-IR Spectra

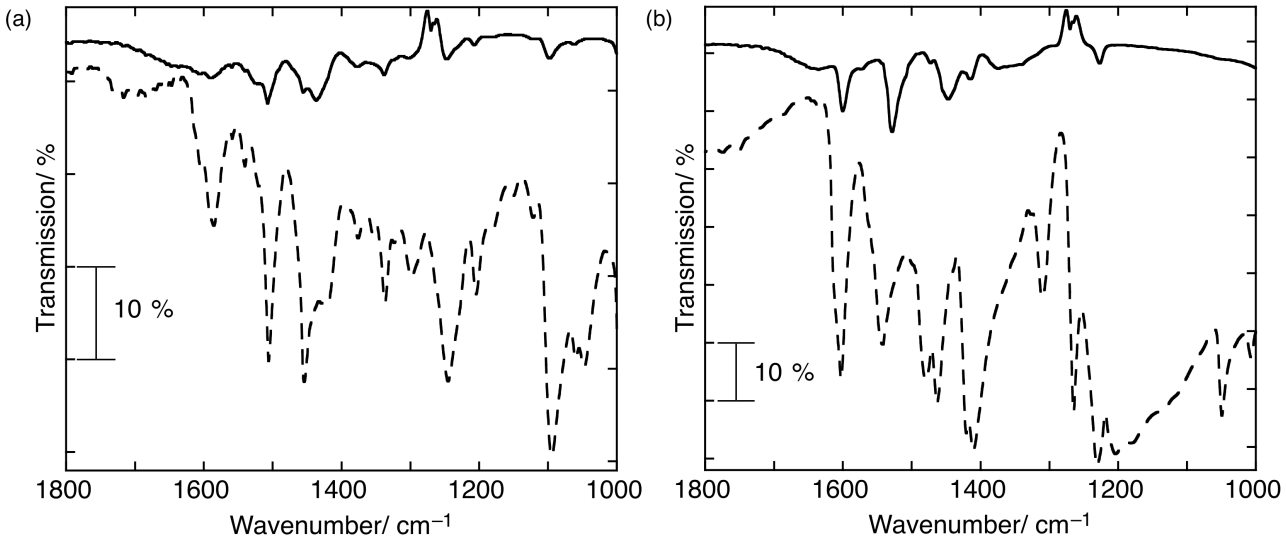

Figure S8. (a) FT-IR spectra of **YD2-*o*-C8T** on TiO_2 (solid) and **YD2-*o*-C8T** powder (dashed). (b) FT-IR spectra of tropolone on TiO_2 (solid) and tropolone powder (dashed).

10. XPS Spectra

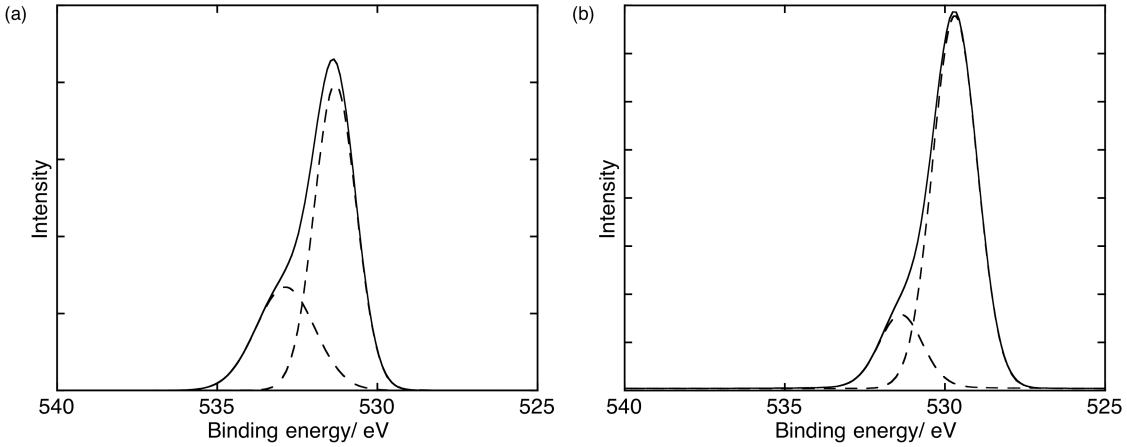

Figure S9. X-Ray photoelectron O1s spectra of (a) tropolone powder and (b) tropolone on TiO_2.

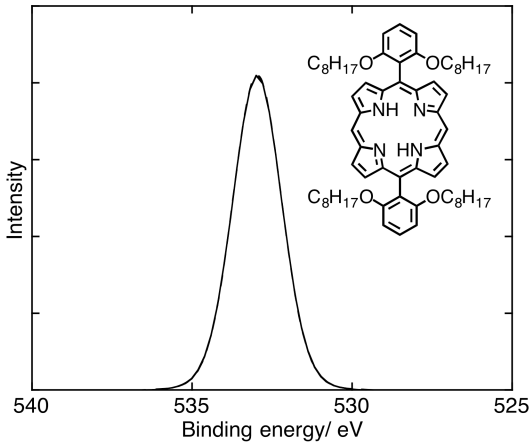

Figure S10. X-Ray photoelectron O1s spectrum of reference porphyrin that is shown as the inset.

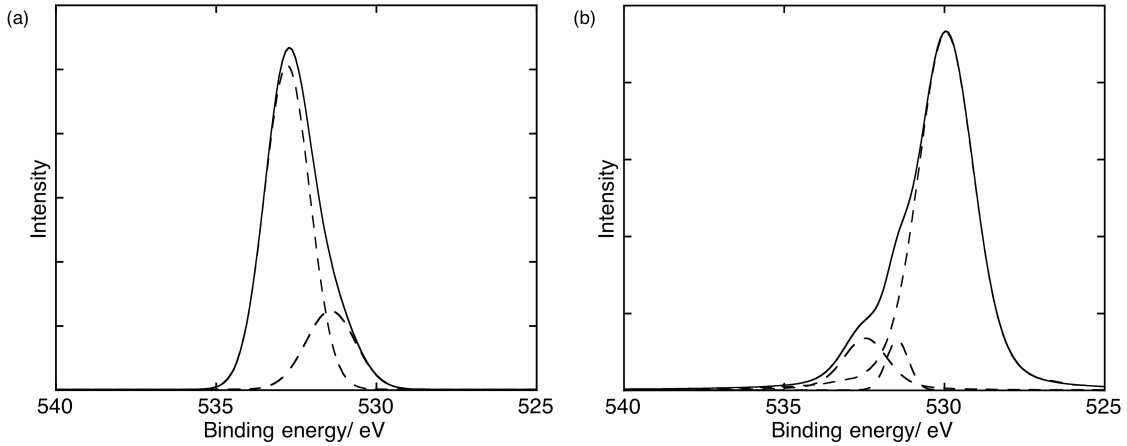

Figure S11. X-Ray photoelectron O1s spectra of (a) **YD2-*o*-C8T** powder and (b) **YD2-*o*-C8T** on TiO_2.

11. Device Optimization

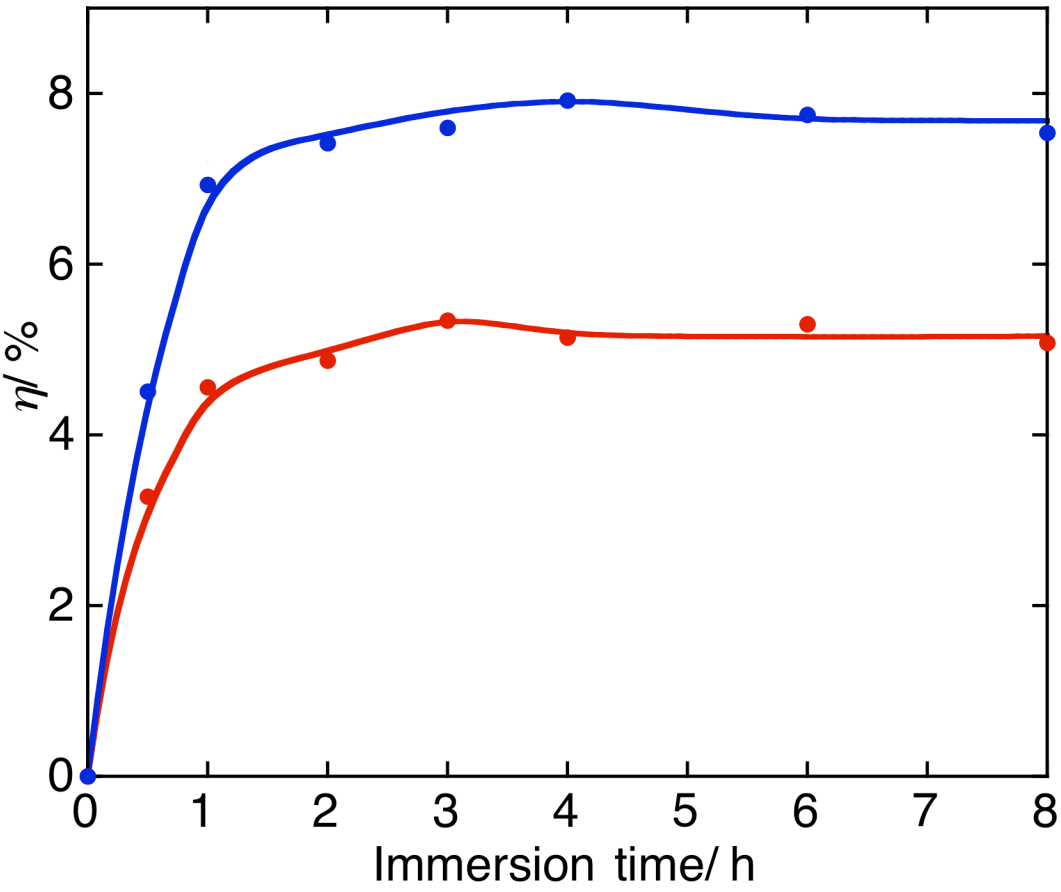

Figure S12. Immersion time profiles of the power conversion efficiency (η) of the DSSCs based on **YD2-*o*-C8T** (red) and **YD2-*o*-C8** (blue). The porphyrins were adsorbed on the TiO_2 electrodes without CDCA.

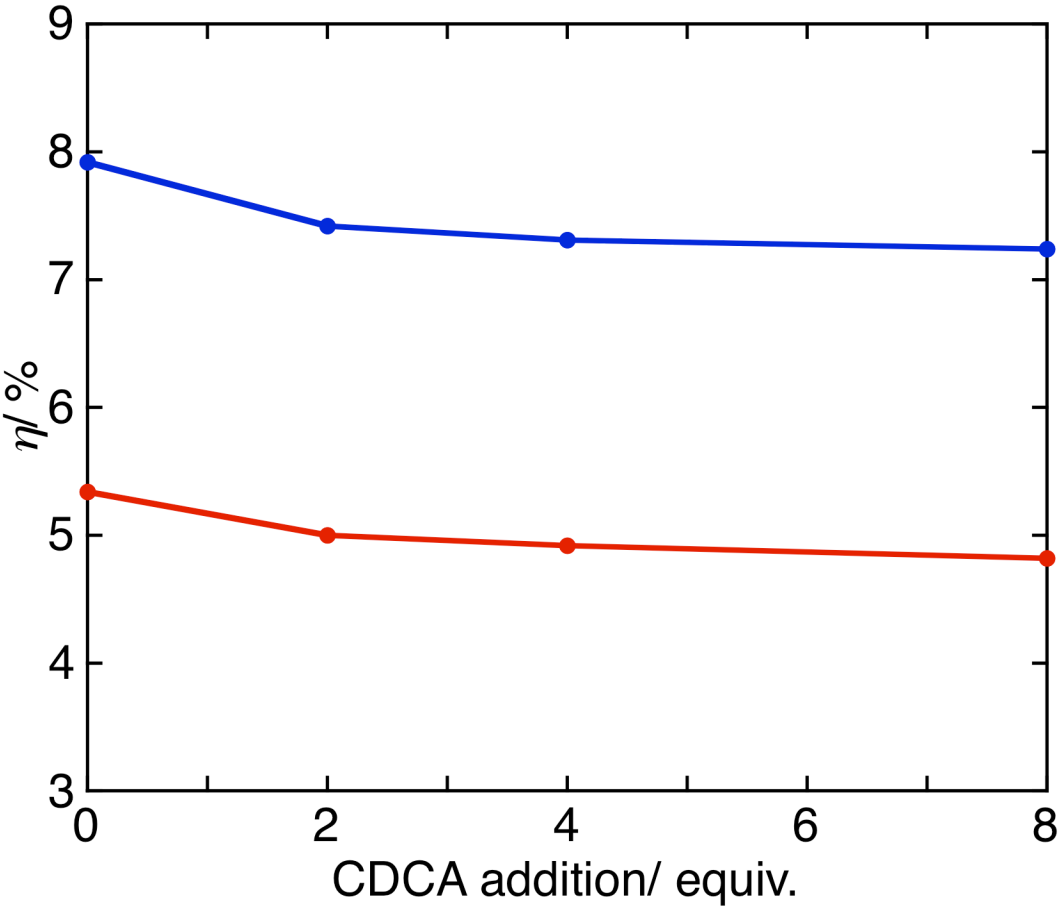

Figure S13. Plots of the power conversion efficiency (η) as a function of the amount of CDCA for the DSSCs based on **YD2-*o*-C8T** (red) and **YD2-*o*-C8** (blue).

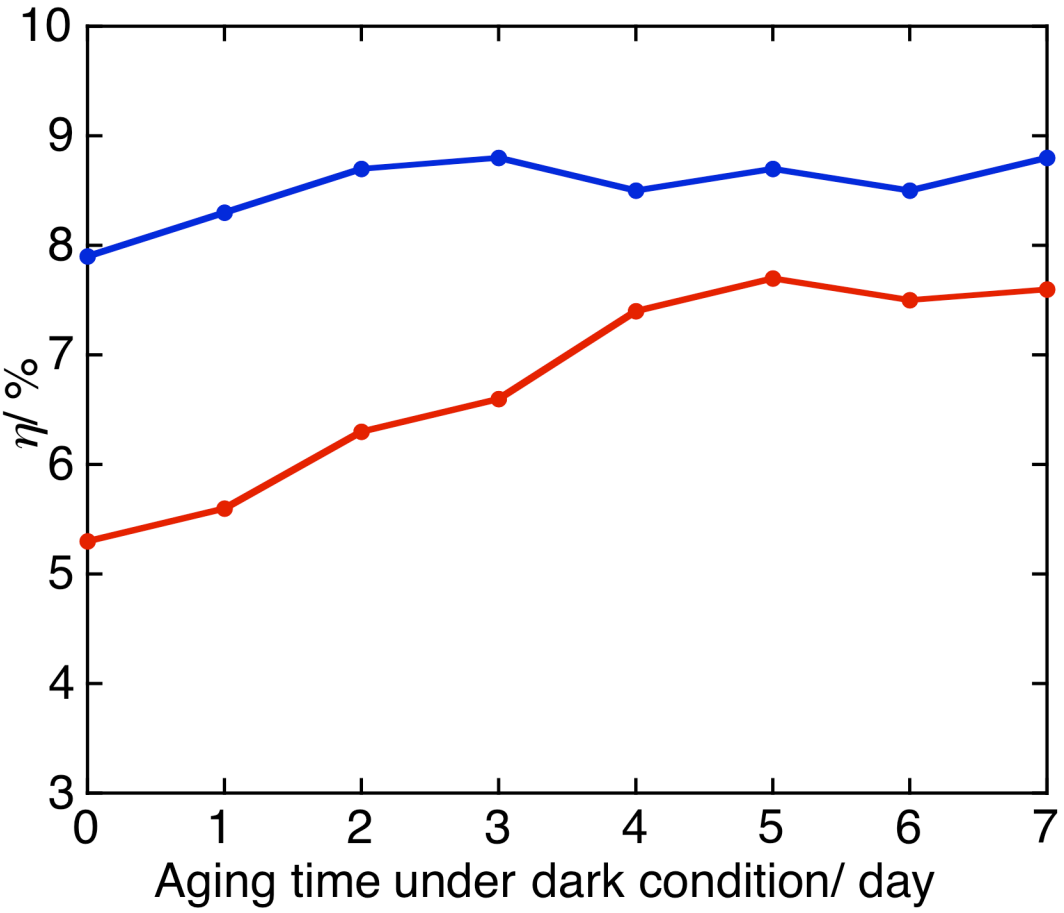

Figure S14. Plots of the power conversion efficiency (η) as a function of aging time for the DSSCs based on **YD2-*o*-C8T** (red) and **YD2-*o*-C8** (blue). The solar cells were kept under dark condition except the period of the photovoltaic measurements. The porphyrin-sensitized TiO_2 electrodes were prepared under the optimized conditions (immersion conditions: 3 h for **YD2-*o*-C8T** and 4 h for **YD2-*o*-C8**).

12. EIS Nyquist Plots

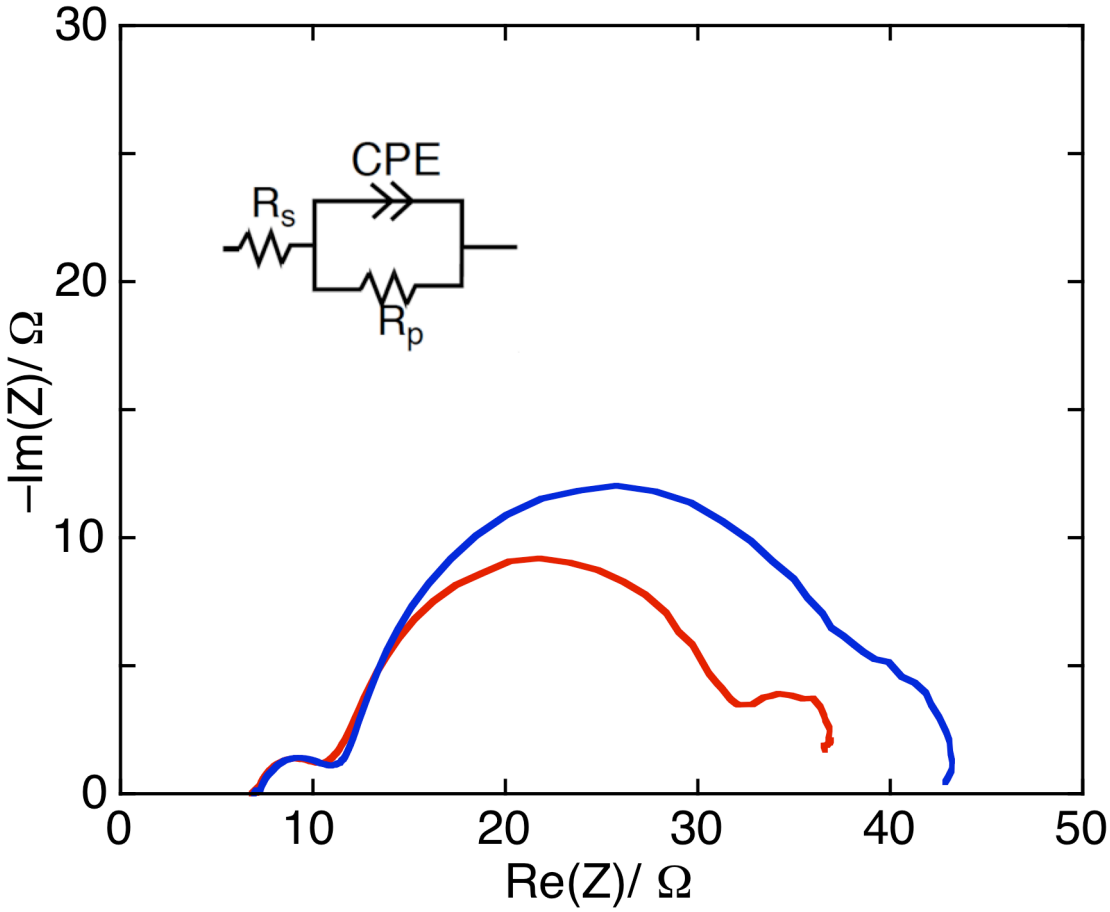

Figure S15. EIS Nyquist Plots of DSSCs based on **YD2-*o*-C8T** (red) and **YD2-*o*-C8** (blue) under AM 1.5 illumination at open-circuit conditions. The inset is an equivalent Randles circuit impedance model. R_S is the series resistance accounting for transport resistance of transparent conducting oxide (TCO); R_p is the charge transfer resistance for charge recombination at the FTO/TiO_2/electrolyte interfaces; while CPE is the constant phase element representing capacitance at the TiO_2/electrolyte/interface. The electron transfer resistances (R_p) at the TiO_2/dye/electrolyte interface were determined as 22.0 Ω for **YD2-*o*-C8T** and 28.7 Ω for **YD2-*o*-C8**.

13. References

[S1] *Gaussian 09*, Revision D.01, M. J. Frisch, G. W. Trucks, H. B. Schlegel, G. E. Scuseria, M. A. Robb, J. R. Cheeseman, G. Scalmani, V. Barone, B. Mennucci, G. A. Petersson, H. Nakatsuji, M. Caricato, X. Li, H. P. Hratchian, A. F. Izmaylov, J. Bloino, G. Zheng, J. L. Sonnenberg, M. Hada, M. Ehara, K. Toyota, R. Fukuda, J. Hasegawa, M. Ishida, T. Nakajima, Y. Honda, O. Kitao, H. Nakai, T. Vreven, J. A. Montgomery, Jr., J. E. Peralta, F. Ogliaro, M. Bearpark, J. J. Heyd, E. Brothers, K. N. Kudin, V. N. Staroverov, T. Keith, R. Kobayashi, J. Normand, K. Raghavachari, A. Rendell, J. C. Burant, S. S. Iyengar, J. Tomasi, M. Cossi, N. Rega, J. M. Millam, M. Klene, J. E. Knox, J. B. Cross, V. Bakken, C. Adamo, J. Jaramillo, R. Gomperts, R. E. Stratmann, O. Yazyev, A. J. Austin, R. Cammi, C. Pomelli, J. W. Ochterski, R. L. Martin, K. Morokuma, V. G. Zakrzewski, G. A. Voth, P. Salvador, J. J. Dannenberg, S. Dapprich, A. D. Daniels, O. Farkas, J. B. Foresman, J. V. Ortiz, J. Cioslowski, D. J. Fox, Gaussian, Inc.; Wallingford CT, **2013**.

[S2] K. Kurotobi, Y. Toude, K. Kawamoto, Y. Fujimori, S. Ito, P. Chabera, V. Sundström, H. Imahori, *Chem. Eur. J.* **2013**, *19*, 17075–17081.

[S3] S. Ito, T. N. Murakami, P. Comte, P. Liska, C. Grätzel, M. K. Nazeeruddin, M. Grätzel, *Thin Solid Films* **2008**, *516*, 4613–4619.

[S4] A. Yella, H.-W. Lee, H. N. Tsao, C. Yi, A. K. Chandiran, M. K. Nazeeruddin, E. W.-G. Diau, C.-Y. Yeh, S. M. Zakeeruddin, M. Grätzel, *Science* **2011**, *334*, 629–634.

[S5] J. Potenziano, R. Spitale, M. E. Janik, *Synth. Commun*. **2005**, *35*, 2005–2016.